

AD-A227 926

| | | | |
|--|--|---|--|
| REPORT DOCUMENTATION PAGE | | Form Approved OMB No. 0704-0188 | |
| | | DTIC FILE COPY | |
| 1. REPORT DATE 14 Jan 85 | | 2. REPORT TYPE AND DATES COVERED Conference Presentation | |
| 3. AUTHOR(s) Interrelated Effects of Pitch Rate and Pivot Point on Airfoil Dynamic Stall | | 5. FUNDING NUMBERS TA 2307-F1-38 | |
| 4. E. Helin and J. M. Walker | | | |
| F.J. Seiler Research Laboratory USAF Academy CO 80840-6528 | | 6. PERFORMING ORGANIZATION REPORT NUMBER FJSRL-PR-90-0002 | |
| | | 7. DISTRIBUTION STATEMENT ADVISORY REPORT NUMBER | |
| Distribution Unlimited | | 8. DISTRIBUTION CODE | |
| <p>Experimental investigations were conducted to study energetic dynamic stall vortices and the associated unsteady aerodynamics generated by a pitching NACA 0015 airfoil. The airfoil model was pitched from zero degrees to 60 degrees at constant pitch rates of 460 deg/sec, 920 deg/sec, and 1380 deg/sec about its quarter-chord, half-chord, and three quarter-chord positions. Extensive 35mm still photographs and 16mm high-speed movies, both employing smoke wire flow visualization, visually documented the initiation and development of the time dependent dynamic stall phenomena. In addition, hot-wire anemometry measurements were made which provided for more quantitative analysis of the unsteady separated flowfields. Pitch rate and pivot point were shown to have interrelated effects on the development of the dynamic stall flowfield. In many cases similar "looking" flowfields were generated by different combinations of pitch rate and pivot point. However, significant differences were observed in the near-surface velocity profiles. <i>Keywords:</i></p> <p>dynamic loads, Pitch motion/vortices aerodynamics flow visualization. (C) 85</p> | | | |
| 9. SECURITY CLASSIFICATION OF THIS PAGE UNCLASSIFIED | | 10. SECURITY CLASSIFICATION OF ABSTRACT UNCLASSIFIED | |
| 11. SECURITY CLASSIFICATION OF ABSTRACT UNCLASSIFIED | | 12. LIMITATION OF ABSTRACT NONE | |

AIAA'85

AIAA-85-0130

Interrelated Effects of Pitch Rate and Pivot Point on Airfoil Dynamic Stall

H. E. Helin and J. M. Walker,
Frank J. Seiler Research Lab.,
USAF Academy, Colorado Springs, CO

| | |
|--------------------|-------------------------------------|
| Accession For | |
| NTIS GRA&I | <input checked="" type="checkbox"/> |
| DTIC TAB | <input checked="" type="checkbox"/> |
| Unannounced | <input type="checkbox"/> |
| Justification | |
| By | |
| Distribution/ | |
| Availability Codes | |
| Dist | Avail and/or Special |
| A-1 | |

AIAA 23rd Aerospace Sciences Meeting

January 14-17, 1985/Reno, Nevada

INTERRELATED EFFECTS OF PITCH RATE AND PIVOT POINT ON AIRFOIL DYNAMIC STALL

Hank E. Helin*
and

John M. Walker**

Frank J. Seiler Research Laboratory
USAF Academy
Colorado Springs, Colorado 80840-6528

Abstract

Experimental investigations were conducted to study energetic dynamic stall vortices and the associated unsteady aerodynamics generated by a pitching NACA 0015 airfoil. The airfoil model was pitched from 0° to 60° at constant $\dot{\alpha}$ rates of $460^\circ/\text{s}$, $920^\circ/\text{s}$ and $1380^\circ/\text{s}$ about its quarter-chord, half-chord, and three quarter-chord positions. Extensive 35 mm still photographs and 16 mm high-speed movies, both employing smoke wire flow visualization, visually documented the initiation and development of the time dependent dynamic stall phenomena. In addition, hot-wire anemometry measurements were made which provided for more quantitative analysis of the unsteady separated flowfields. Pitch rate and pivot point were shown to have interrelated effects on the development of the dynamic stall flowfield. In many cases similar "looking" flowfields were generated by different combinations of pitch rate and pivot point. However, significant differences were observed in the near-surface velocity profiles.

Introduction

The energetic nature of the unsteady flowfields generated by pitching airfoils have been a topic of study for much of the 20th century.¹ The vast number and interaction of variables involved have significantly complicated both theoretical and experimental efforts to understand the fluid mechanics and the development of reliable prediction methods. Most theoretical studies revolve around attempts to relax assumptions postulated in steady thin airfoil theory. In general, the results from these studies have been somewhat restricted and significant progress has been elusive. This is due in part to the

lack of broad scope experimental data which are needed to set modeling parameters and as a basis for checking theoretical calculations. The general thrust of experimental unsteady aerodynamic research has been to reduce the undesirable effects associated with dynamic stall. Many of the parameters involved have been restricted to model specific areas and types of problems. However, with the more recent realization that the extremely energetic nature of unsteady flows might be exploited and utilized to enhance performance, the scope of research efforts have been expanded significantly.²

Unsteady aerodynamic effects generated by pitching or oscillating airfoils are generally classified under the heading of "Dynamic Stall." Inherent in this phenomenon is the development of a dynamic stall vortex which occurs as the lifting surface dynamically surpasses its static stall angle of attack. Large unsteady aerodynamic forces are generated from which the lift, drag and moment coefficients are seen to greatly exceed their maximum static counterparts.³ The unsteady effects of dynamic stall are dominated by turbulent flow and the production of large scale vortices. The more general methods employed in analyzing dynamic stall involved tests with airfoils driven through moderately large amplitude, slow oscillations in angle of attack. This was in line with attempts to understand and eliminate the undesirable effects associated with dynamic stall on helicopter rotors. In contrast, recent efforts are now also exploring possibilities of utilizing the unsteadiness of the flowfield to enhance performance. These studies have examined new parameter combinations including much higher oscillation/pitch rates.² Studies have been performed to analyze the repetitive interaction of the dynamic stall vortices as a means of maintaining flow attachment (and, hence greatly increasing lift) at high angles of attack.⁴ In addition, extensive studies have also been done to correlate this phenomenon as a function of the driving parameters involved, i.e., pivot location, airfoil shape, Reynolds number, and mean angle of attack.⁵

*Lieutenant, USAF

Instructor, Department of Aeronautics
USAF Academy, Colorado Springs, CO
Member AIAA

**Major, USAF

Aeromechanics Division, FJSRL
USAF Academy, Colorado Springs, CO
Member AIAA

Large, energetic vortical structures have been shown to be an important correlate of oscillating/pitching airfoils, and current research activities have documented their dramatic impact on the lift and drag characteristics.^{6,7} In addition, the impetus to exploit the energetic nature of large vortices as a potential to enhance performance has already been demonstrated.¹ However, it is clearly evident that before such a realistic utilization is possible, extensive studies must be performed to expand our knowledge concerning fundamental aspects. Questions regarding the direct relationship between the time dependent fluid dynamics and associated airfoil/flowfield interaction, have yet to be answered. Before attempts to utilize these phenomena are made, the flowfield dependence upon the driving parameters of airfoil geometry and dynamics must be fully understood. The present study focuses only on a small part of this problem: the relationships between the pitch rate, pitch axis and resultant vortex development.

Methods

Experiments were conducted using a NACA 0015 airfoil model in the USAF Academy's subsonic wind tunnel. Two experimental techniques were employed: (1) smoke-wire flow visualization using 35 mm still and 16 mm high-speed movie cameras, and (2) near-surface hot-wires mounted in a staggered array on the airfoil's surface.

The airfoil model was a NACA 0015 extruded aluminum section with a 6" chord and 22" span. The airfoil was pitched from 0° to 60° by a single-degree-of-freedom oscillator employing a DC stepping motor and an index controller which was computer driven. Airfoil angular position was measured by a linear potentiometer mounted on the oscillator. System performance checks documented cycle to cycle repeatability with a maximum standard deviation of 0.5° over a 25 run ensemble average.

The USAF Academy's subsonic wind tunnel has a 2'x3' test section. All testing was conducted at a freestream velocity of 20 ft/s which, with the 6" NACA 0015, resulted in an airfoil Reynolds number of 45,000. The turbulence intensity level of the tunnel in this velocity range has been documented at less than 0.1%. The low turbulence level and the low velocity were necessary for high quality detailed flow visualization.

Flow visualization was obtained using a .005" tungsten wire coated with theatrical fog fluid. An electrical

current was applied to the wire which produced a set of fine streaklines across the test section. These streaklines were photographed using a high intensity arc-lamp strobe light, with a flash duration of 7 μ s, coupled with a 35 mm camera and a 16 mm high-speed movie camera. The 35 mm photographs are phase-locked single exposure on 400 ASA TRI-X film developed at 1200 ASA. Only one photograph could be taken during a pitch motion which required multiple motion sequences with each successive photograph at an incremented angle of attack. The 16 mm high-speed camera system, however, allowed multiple photographs over one motion cycle, which provided for detailed studies of the flowfield evolution as a function of time. The entire oscillator/smoke-wire/flash/camera system was controlled and synchronized using a PDP 11/45 and PDP 11/03 computer system.

Near surface velocity measurements were made using seven hot-wires mounted on the upper (suction) surface of the airfoil. The hot-wire sensing elements (TSI-10 Hotfilms) were fixed at .2" above the surface and equally spaced at .8" increments. The sensor positions were .4", 1.2", 2.0", 2.8", 3.6", 4.4", and 5.2" on the 6" chord airfoil. Velocity signals were obtained using a TSI 1050 anemometer system coupled with the Laboratory Peripheral System package of the PDP 11/45 computer. The velocities at the various sensor locations, with the airfoil at 0° angle of attack, were compared with a freestream hot-wire to obtain normalizing coefficients. The measured velocities over the airfoil surface were in turn normalized to a percent of freestream for analysis. The sampling rate varied with the pitch rate employed but was always above 1 KHz.

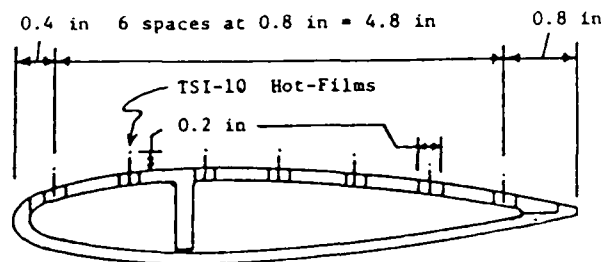


Figure 1. Surface Hot-Wire Configuration

Results

A well known effect of oscillating or pitching an airfoil is that the static stall angle can be exceeded by some amount before dynamic stall occurs. Dynamic stall is preceded by the separation of flow near the trailing edge. This forms a separated region over the airfoil which grows rapidly as its

initiation point moves up from the trailing edge toward the leading edge. As the airfoil stalls dynamically, a large vortex is shed from near the leading edge. The initiation, development, and even the strength of the dynamic stall vortex, have been shown to be a complex function of the driving parameters. This function is far from being fully understood. Rather than complicate the scheme further by using periodic motions, which set up a hysteresis loop, constant pitch motions from 0° up to a angle of attack of 60° were employed. Once the maximum angle was reached the airfoil was stopped, allowing the unsteady flowfields to develop freely.

A steady state study of static stall conditions for the NACA 0015 airfoil was conducted. As the airfoil was slowly incremented toward the static stall angle under steady flow conditions, a trailing edge separation zone formed and moved up the suction surface of the airfoil until, at an angle of attack of 12° , flow was separated over fifty percent of the airfoil chord. This was readily determined by smoke flow visualization. This steady flow stall criterion will be used to compare the delay in onset of dynamic stall with regard to angle of attack and the initiation of the dynamic stall vortex. Qualitative analyses of flow visualization are based upon the initiation of the dynamic stall vortex, its temporal position with respect to the airfoil angle of attack which is dependent on the pitch rate employed, and its spatial position with respect to the airfoil chord. These analyses are compared and correlated with the near surface velocities measured with the hot-wires.

Table 1 shows the combinations of pitch rates and pitch axes that were employed. These combinations of driving variables allowed for analyses of the initiation and development of unsteady dynamic stall flowfields based upon chord angular displacement with respect to time, airfoil leading edge angular velocities, and the interrelated effects of chord and leading edge angular velocities.

Table 1. Pitch Rates and Pitch Axes

| | PITCH RATE | | |
|-------|----------------------|----------------------|-----------------------|
| | $460^\circ/\text{s}$ | $920^\circ/\text{s}$ | $1380^\circ/\text{s}$ |
| 0.25c | X | X | X |
| 0.5c | | X | |
| 0.75c | | X | |

Increased Pitch Rate, Fixed Pitch Axis

With the pitch axis fixed at 0.25 c the dramatic effects of increased pitch rate are visually documented in Figure 2. As the pitch rate was increased from $460^\circ/\text{s}$ to $920^\circ/\text{s}$, and finally to $1380^\circ/\text{s}$, the initiation of the dynamic stall vortex was delayed to higher angles of attack. This delay is not a linear function of the pitch rate. The effects of an increment in pitch rate are more prominent at lower rates than at higher rates. At a pitch rate of $460^\circ/\text{s}$ the dynamic stall vortex began to form around 22° . At double the pitch rate, $920^\circ/\text{s}$, it began forming at 31° . However, an increase to $1380^\circ/\text{s}$ only pushed the dynamic stall vortex initiation to 34° . Another dominant feature is the spatial position of the vortex with respect to the airfoil. At the lower pitch rates the vortex formed much earlier in the pitch cycle and moved rapidly downstream. As the pitch rate increased, the dwell time that the vortex remained close to and over the airfoil also increased. In all cases, the dynamic stall vortex remained energetic and continued to rotate until well downstream of the airfoil. This is not readily discernible from still photographs taken over multiple cycles, but was clearly evident in the high-speed 16 mm movies taken over a single cycle.

The 16 mm movies taken at 500 frames per second visualized the dramatic differences between streaklines and streamlines for a time dependent flowfield. Many of the contorted streaklines were seen to develop early as the vortex was forming, and then were carried along as historical patterns. However, the energetic rotation of the vortex was easily seen from frame to frame and the streaklines are indicative of the vortex position and temporal development. In addition, the movies document the direction of the flow at different points in the flowfield. This was very useful in determining rotational directions and reverse flow areas over the surface.

When the movies are compared to the still photographs and hot-wire data, with respect to angle of attack, a quantitative analysis of the flowfield and vortex development is easily made. Since the hot-wire sensors are close to the surface they indicate the magnitude of the flow which is essentially parallel to the surface. And, when correlated with the flow visualization, the direction of the flow along the surface is readily discernible much of the time. Peaks in the profiles match with the spatial positions, as observed in the flow visualization, of the vortex centers

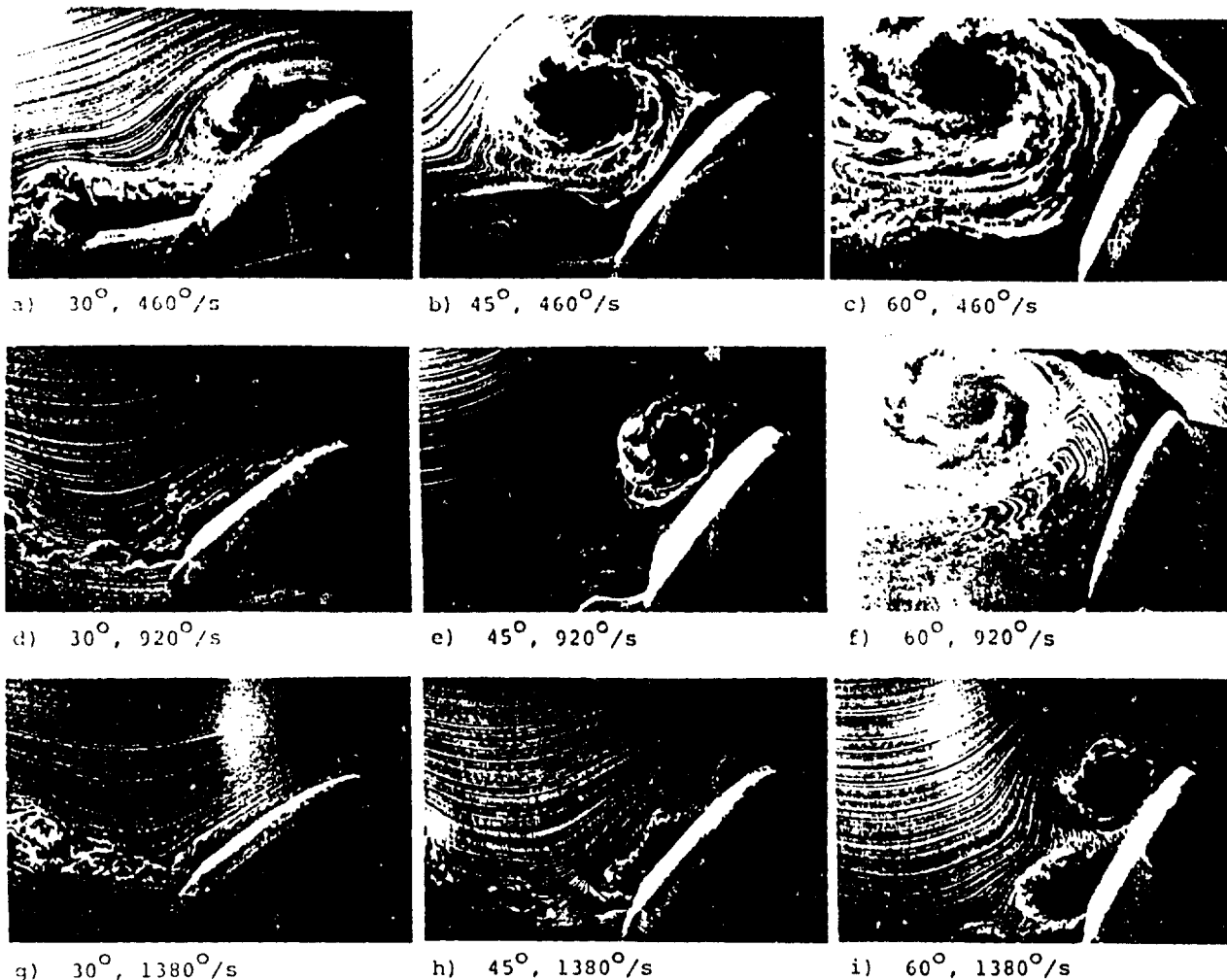


Figure 2. Pitch Rates of $460^\circ/\text{s}$, $920^\circ/\text{s}$, and $1380^\circ/\text{s}$ with Pictures at 30° , 45° , and 60° for Each Rate. Pitch Axis Constant at $0.25c$.

over the airfoil. Figure 3 shows the velocities in percent freestream at the first sensor location for the three different pitch rates. Peaks in the velocity profiles at the first sensor agree with the vortex initiation angles documented in the flow visualization. It is interesting to note that the slope of the velocity profiles, up to the point of vortex initiation, as a function of the angle of attack is relatively independent of the pitch rate. Another interesting feature is that the maximum velocity of the first sensor was also seen to be independent of the pitch rate, as evidenced by the near equal magnitudes of the peaks in Figure 3. However, the relative magnitude of the velocities at stations further aft are different for changes in pitch rate.

Correlation of peaks in the velocity profiles with observed vortex positions from the flow visualizations showed that the maximum velocities increase as the

pitch rate was increased. An example of this is in Figure 4, which shows the magnitude of the velocity at sensor number 2, on the suction surface of the airfoil for two different pitch rates. These higher velocities, and the fact that the flow visualization also showed more cohesive appearing vortices as the pitch rate was increased, are a direct inference to an increase in vortex strength as a function of increasing pitch rate. This readily suggests that the increased dwell time at the higher pitch rates is directly coupled to the increased energetic and cohesive nature of the dynamic stall vortices at the higher pitch rates.

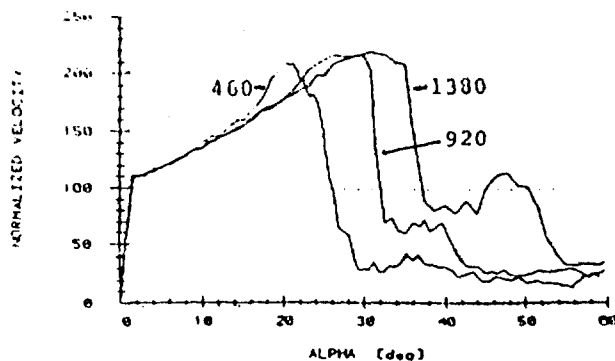


Figure 3. Magnitude of the Velocities at Sensor Number One, in Percent Freestream, for Pitch Rates of 460°/s, 920°/s and 1380°/s. Pitch Axis is 0.25c.

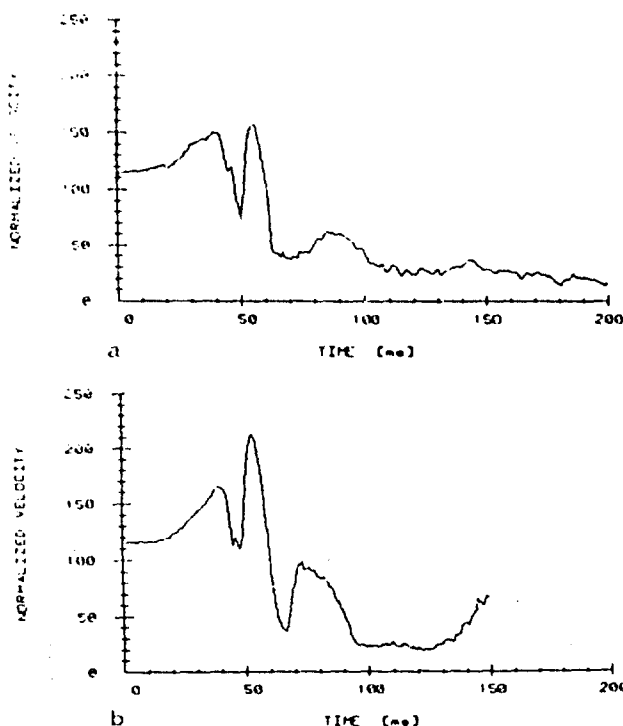


Figure 4. Magnitude of the Velocities over the Airfoil Surface, in Percent Freestream, at Sensor Number Two. Pitch Axis is .25 c. Pitch Rate is a) 920°/s, b) 1380°/s.

Increased Pitch Axis, Pitch Rate Constant

As shown by the flow visualization photographs in Figure 5, the effects of moving the pitch axis further along the chord are similar to those discovered for

increasing pitch rate. As the distance from the leading edge was increased from 0.25 c to 0.5 c and finally 0.75 c, the onset of dynamic stall was again delayed. Once the leading edge vortex was generated, its evolution and growth characteristics during the remaining portion of the pitch cycle, and with time, appeared constant.

Although the initiation of the dynamic stall vortex was delayed to very high angles of attack, the subsequent rapid development and movement of the vortex over the airfoil was very similar, with no appreciable increase in dwell time regardless of the pitch axis location. This is in contrast to the coupled effect of delayed initiation and increased dwell time as pitch rate was increased. In addition, there is not a perceivable increase in coherent appearance with increased pitch axis distance, as there was with increased pitch rate (Figures 2 and 5). Again, the high-speed 16 mm movies documented the energetic nature of the dynamic stall flowfield, showing continued growth and significant rotation throughout the time the vortex was in the vicinity of the airfoil.

Dynamic stall at the first hot wire sensor, evidenced by sharp decrease in the magnitudes of the velocities shown in Figure 6, occurs at 30°, 36°, and 42° for pitch axes of 0.25 c, 0.5 c and 0.75 c, respectively. This represents a relatively linear increase in stall delay as a function of increased pitch axis distance. Figure 6 is also illustrative of significant differences in the velocity magnitude profiles at the first sensor location. There is a definite decrease in the slope, with respect to angle of attack, as the pitch axis distance from the leading edge was increased. Also, the peak velocity at the first sensor decreased as pitch axis was increased - more so from 0.25 c to 0.5 c than from 0.5 c to 0.75 c. These two phenomena are completely different from observations at increasing pitch rate (Figure 3).

As mentioned in the flow visualization discussion, the development of the stall flowfield appears quite similar, except for an increase in the dynamic stall angle, regardless of the pitch axis employed. The remarkable similarities in the velocity profiles as a function of time, at sensor number three, are shown in Figure 7 for the three pitch axes. As pitch axis distance was increased, the initial slopes decreased slightly (as noted before at sensor number one), the maximum magnitude of the peaks decreased slightly, and dynamic stall was delayed. However, the

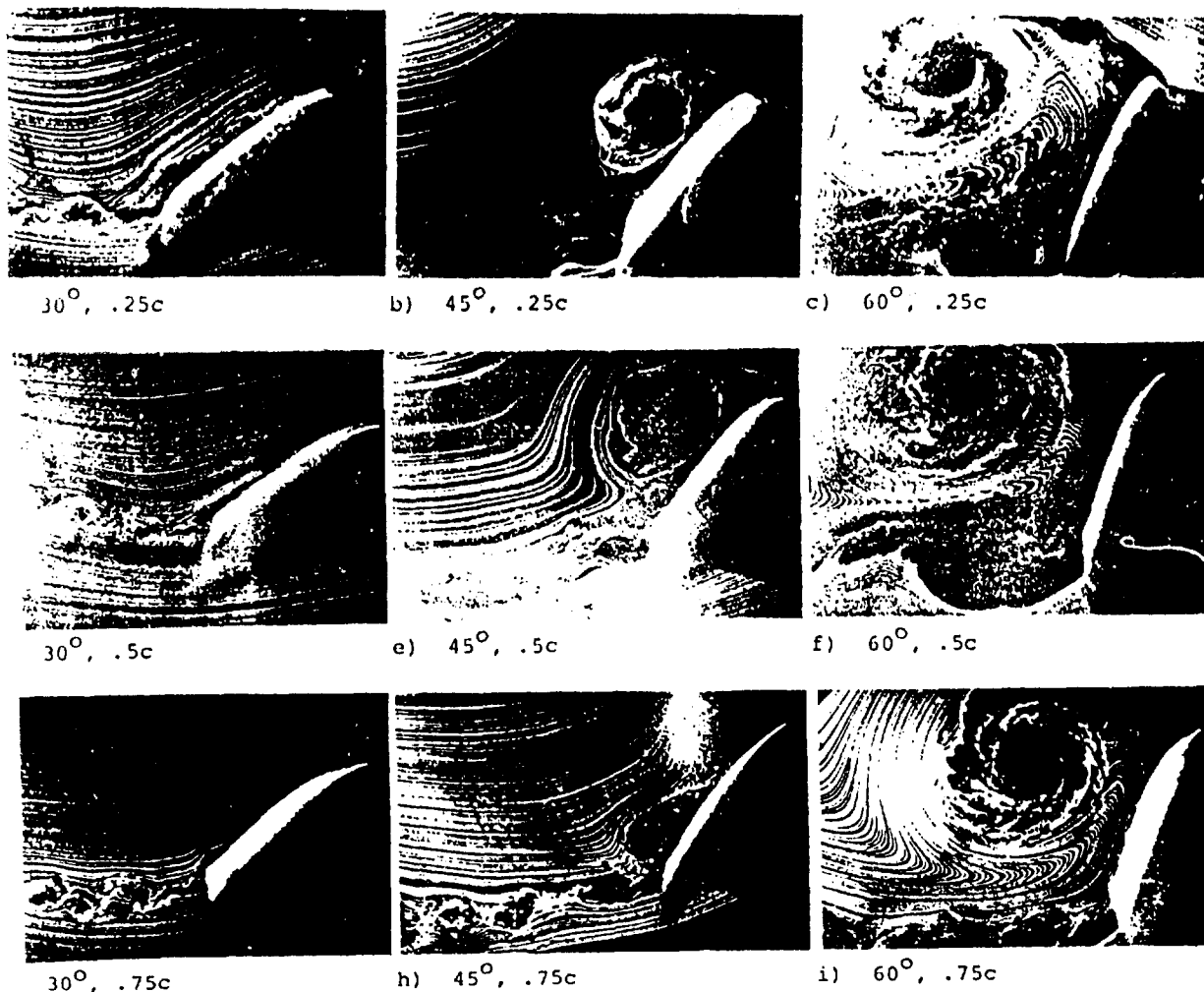


Figure 5. Pitch Axes of 0.25 c, 0.5 c and 0.75 c with Pictures at 30° , 45° and 60° for each axes. Pitch Rate Constant at $920^\circ/\text{s}$.

neral shape of the profiles are overwhelmingly similar and are merely lifted an increment of time as the pitch is moved aft.

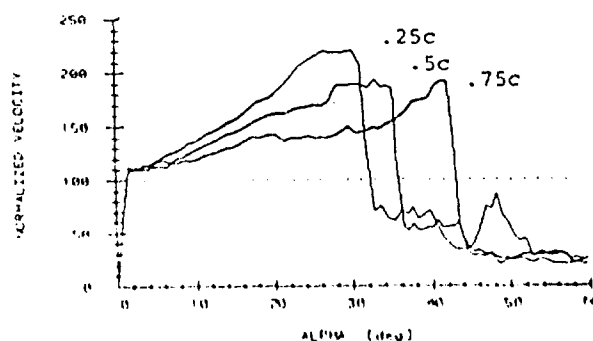


Figure 6. Magnitude of the Velocities at Sensor Number One, in Percent Freestream, for Pivot Axes of 0.25 c, 0.5 c and 0.75 c. Pitch Rate is $920^\circ/\text{s}$.

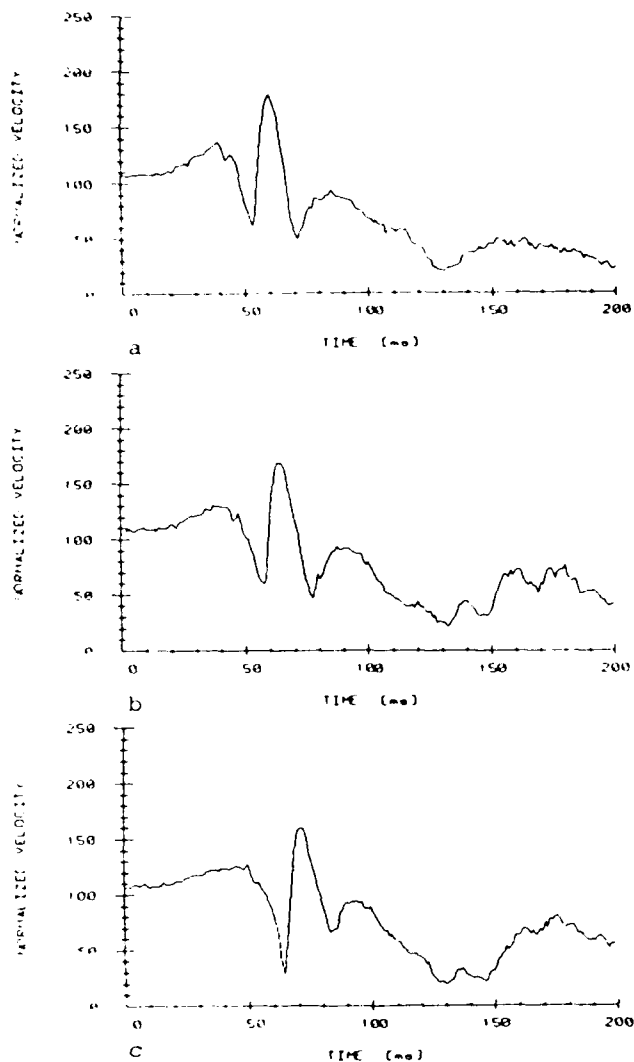


Figure 7. Magnitude of the Velocities over the airfoil surface, in Percent Freestream, at Sensor Number Three. Pitch Rate is $920^\circ/\text{s}$. Pitch Axis is a) 0.25c, b) 0.5c, c) .75c.

Discussion

Studies of an airfoil pitched from 0° to 60° angle of attack, at various pitch rates about different pitch axes, have shown the development of a complex interactive flowfield. The most prevalent feature was the formation of an energetic dynamic stall vortex which both spatially and temporally dependent on the driving parameters. The dynamic stall phenomenon was extremely reproducible. In light of this reproducible nature, single shot photographs, over many motion cycles, and ensemble averaged hotwire profiles were used to quantify flowfield development. In addition, high speed movies documented the energetic rotation

and travel of the dynamic stall vortex as it developed. The presence of the dynamic stall vortex was observed to have significant effect on the velocity distribution over the airfoil surface at angles of attack well beyond the normal static stall.

As the dynamics of the airfoil motion were changed, the following impacts on the dynamic stall process were observed: 1) Pitch Rate - It is clearly evident that as the pitch rate is increased, the angle of attack at which dynamic stall occurs is also increased. This effect is nonlinear and more prevalent at increments in low pitch rates than at the higher rates. In fact, although using a different range of parameters, Gormont suggests that this goes as the square root of the pitch rate.⁸ In addition, the slope of the velocity profile with respect to angle of attack, close to the surface and near the leading edge, does not change as the pitch rate is increased. Also, the corresponding peak velocities near the leading edge change very little. There are direct indications that increased pitch rates form more coherent and energetic dynamic stall vortices. As the vortices become more energetic, (as was shown by increased velocity magnitudes in the profiles aft of the leading edge), they remain over the airfoil for a longer period of time. This would dramatically influence the time averaged aerodynamic forces on the airfoil at high angles of attack.

2) Pitch Axis - Moving the pitch axis toward the trailing edge emulates some of the effects of an increased pitch rate. Dynamic stall occurs at correspondingly higher angles of attack, and the large dynamic stall vortex again has significant impact on the velocities over the airfoil surface. However, differences do exist in the velocity profiles and vortex dynamics from those noted for an increased pitch rate. The slope of the velocity magnitude profiles at the first sensor changed substantially; the velocity increased at a slower rate and did not reach as high a peak when the pitch axis was moved toward the trailing edge. Also, the dynamic stall vortex, once initiated, evolved rapidly and moved quickly downstream regardless of the pitch axis. Substantial similarities were seen in the velocity magnitude profiles of the mid-chord region for the various pitch axis locations. The profiles had the same relative peaks and magnitudes, with the only difference being a slight temporal increment as the pitch axis was moved aft.

These observed phenomena show the dramatic effects of pitch rate and pitch axis on the dynamic stall process. Clearly, more quantitative aerodynamic measurements are needed to precisely select an optimal parameter combination to enhance performance. Experimental studies to quantify these and other effects are underway using more extensive hot-wire techniques and miniature surface mounted pressure transducers.

References

1. McCroskey, W.J., "Unsteady Airfoils," Annual Review of Fluid Mechanics, 1982, pp. 285-311.
2. Robinson, M.C. and Luttges, M.W., "Unsteady Separated Flow: Forced and Common Vorticity About Oscillating Airfoils." Workshop on Unsteady Separated Flows, 10-11 Aug 1983, U.S. Air Force Academy. Proceedings pp. 117-126.
3. Carr, L.W., McAlister, K.W., and McCroskey, W.J., "Analysis of the Development of Dynamic Stall Based on Oscillating Airfoil Experiments," NASA TN D-8382, Jan 1977.
4. Robinson, M.C., and Luttges, M.W., "Vortex Generation Induced by Oscillating Airfoils: Maximizing Flow Attachment," 8th Biennial Symposium on Turbulence, Rolla, MO, 26-28 Sep 1983, pp. 13.1-13.10.
5. Robinson, M.C. and Luttges, M.W., "Unsteady Flow Separation and Reattachment Induced by Pitching Airfoils," AIAA Paper No. 83-0131, Jan 1983, pp. 1-14.
6. McCroskey, W.J., et. al., "Dynamic Stall Experiments on Oscillating Airfoils," AIAA Paper No. 75-125, Jan 1975.
7. Martin, J.M., Empey, R.W., McCroskey, W.J., and Cardonna, F.X., "Experimental Analysis of Dynamic Stall on an Oscillating Airfoil," Journal of the American Helicopter Society, Vol. 19, No. 1, Jan 1973, pp. 26-32.
8. Gormont, R.E., "A Mathematical Model of Unsteady Aerodynamics and Radial Flow for Application to Helicopter Rotors," U.S. Army AMRDL Technical Report 72-67, 1973.